

End-to-End Distribution Function of Two-Dimensional Stiff Polymers for all Persistence Lengths

B. Hamprecht¹, W. Janke² and H. Kleinert¹

¹ *Institut für Theoretische Physik, Freie Universität Berlin,
Arnimallee 14, D-14195 Berlin, Germany*

² *Institut für Theoretische Physik, Universität Leipzig,
Augustusplatz 10/11, D-04109 Leipzig, Germany*

e-mail: bodo.hamprecht@physik.fu-berlin.de e-mail: wolfgang.janke@itp.uni-leipzig.de e-mail: hagen.kleinert@physik.fu-berlin.de

We set up and solve a recursion relation for all even moments of a two-dimensional stiff polymer (Porod-Kratky wormlike chain) and determine from these moments a simple analytic expression for the end-to-end distribution at all persistence lengths.

I. INTRODUCTION

In a recent note [1], two of us set up a recursion relation for the even moments of the end-to-end distribution of stiff polymers in D dimensions and used the resulting moments of high order to construct a simple analytic distribution function of the end-to-end distance \mathbf{R} . For large persistence length ξ , the result agrees well with perturbative and Monte Carlo results of Wilhelm and Frey [2], for small ξ with the Daniels correction [3].

Recently, Dahr and Chaudhuri [4] have pointed out the existence of an interesting dip-structure in the distribution function for two dimensions appearing at intermediate ξ -values in the *spatial* density function $P_L(\mathbf{R}) \equiv P_L(R)/R$ normalized to unity as $\int d^2x P_L(\mathbf{R}) = 1$. The often-plotted *radial* density function $P_L(R)$ with the normalization $\int P_L(R) dR = 1$ makes this dip almost invisible. If one wants this dip to show up in a simple analytic approximation of the type in Ref. [1], several more parameters are needed. The purpose of this note is to construct such an analytic expression which fits excellently high-precision Monte Carlo data.

The end-to-end distribution function of a stiff polymer in two dimensions is given by the path integral [5]

$$P_L(\mathbf{R}) \propto \int d\phi_b d\phi_a \mathcal{D}\phi(s) e^{-E_b/k_B T} \delta^{(2)}\left(\mathbf{R} - \int_0^L ds \mathbf{u}(s)\right) \quad (1.1)$$

with the bending energy

$$E_b = \frac{\kappa}{2} \int_0^L ds [\mathbf{u}'(s)]^2. \quad (1.2)$$

where $\mathbf{u}(s) = (\cos \phi(s), \sin \phi(s))$ are the direction vectors of the polymer links, and κ is the stiffness which defines the persistence length $\xi \equiv 2\kappa/k_B T$. Due to the presence of the $\delta^{(2)}$ -function in the integrand, the path integral is not exactly solvable. It is, however, easy to find arbitrarily high even moments of the radial distribution of the end-to-end distance $P_L(R)$:

$$\langle R^{2n} \rangle \equiv \int dR R^{2n} P_L(R). \quad (1.3)$$

This was explained for D -dimensions in Ref. [1]. In two dimensions, the moments (1.3) can be obtained from the coefficient of $\lambda^{2n}/2^{2n}(2n)!$ in the expansion of the integral

$$f(\tau; \lambda) \equiv \int_0^\pi d\theta \psi(\theta, \tau; \lambda), \quad (1.4)$$

in powers of λ , evaluated at the euclidean time $\tau = \xi$. Here we use natural units with $L = 1$. The wave function $\psi(\theta, \tau; \lambda)$ is a solution of the Schrödinger equation in euclidean time

$$\hat{H}\psi(\theta, \tau; \lambda) = -\frac{d}{d\tau}\psi(\theta, \tau; \lambda), \quad (1.5)$$

where

$$\hat{H} = -\frac{1}{2}\Delta + \frac{1}{2}\lambda z \equiv -\frac{1}{2}\frac{d^2}{d\theta^2} + \frac{1}{2}\lambda \cos \theta. \quad (1.6)$$

II. RECURSIVE SOLUTION OF THE SCHRÖDINGER EQUATION.

The function $f(L; \lambda)$ has a spectral representation

$$f(L; \lambda) \equiv \sum_{l=0}^{\infty} \frac{\int_0^\pi d\theta \varphi^{(l)\dagger}(\theta) \exp(-E^{(l)}L) \varphi^{(l)}(0)}{\int_0^\pi d\theta \varphi^{(l)\dagger}(\theta) \varphi^{(l)}(\theta)}, \quad (2.1)$$

where the $\varphi^{(l)}(\theta)$ are arbitrarily normalized eigenfunctions of the time-independent interacting Schrödinger equation $\hat{H}\varphi^{(l)}(\theta) = E^{(l)}\varphi^{(l)}(\theta)$. Applying perturbation theory to this problem, we start from the eigenstates $|l\rangle$ of the unperturbed Hamiltonian $\hat{H}_0 = -\Delta/2$, with eigenvalues $E_0^{(l)} = l^2/2$, and form the eigenfunctions $\varphi^{(l)}(\theta) = \langle \theta | l \rangle$ with the explicit form $\varphi^{(0)}(\theta) = 1/\sqrt{4\pi}$ and $\varphi^{(l)}(\theta) = \cos(l\theta)/\sqrt{\pi}$. Note that the ground state wave function is not normalized to unity on purpose, for later convenience. Now we set up a recursion scheme for the expansion coefficients $\gamma_{l',i}^{(l)}$ and $\epsilon_j^{(l)}$ of the eigenfunctions and their energies:

$$|\varphi^{(l)}\rangle = \sum_{l',i=0}^{\infty} \gamma_{l',i}^{(l)} \lambda^i |l'\rangle, \quad E^{(l)} = \sum_{j=0}^{\infty} \epsilon_j^{(l)} \lambda^j. \quad (2.2)$$

The procedure is described in [1, 6]. The properties of the unperturbed system for $\lambda = 0$ determine the initial conditions for the recursion:

$$\gamma_{l,i}^{(l)} = \delta_{i,0}, \quad \gamma_{k,0}^{(l)} = \delta_{l,k}, \quad \epsilon_0^{(j)} = j^2/2. \quad (2.3)$$

To proceed, we need the the matrix elements of the perturbing Hamiltonian \hat{H}_I in the basis of the unperturbed eigenstates. They are simply $\langle n | \hat{H}_I | n \pm 1 \rangle = \lambda/2$. Inserting the expansions (2.2) into the Schrödinger equation (1.5), projecting the result onto some base vector $\langle k |$, and extracting the coefficient of λ^i , we obtain the following recursion relations:

$$\epsilon_i^{(0)} = \gamma_{1,i-1}^{(0)}, \quad \epsilon_i^{(l)} = (\gamma_{l+1,i-1}^{(l)} + \gamma_{l-1,i-1}^{(l)})/2, \quad (2.4)$$

and

$$\gamma_{0,i}^{(l)} = \frac{2}{l^2} \left(\gamma_{1,i-1}^{(l)} - \sum_{j=1}^{i-1} \epsilon_j^{(l)} \gamma_{0,i-j}^{(l)} \right), \quad (2.5)$$

$$\gamma_{k,i}^{(l)} = \frac{1}{l^2 - k^2} \left(\gamma_{k+1,i-1}^{(l)} + \gamma_{k-1,i-1}^{(l)} - 2 \sum_{j=1}^{i-1} \epsilon_j^{(l)} \gamma_{k,i-j}^{(l)} \right). \quad (2.6)$$

Starting from the initial values (2.3), these recursion relations determine successively the higher-order expansion coefficients in (2.2). Inserting the resulting expansions (2.2) into Eq. (2.1), only the constant parts in $\varphi^{(l)}(\theta)$ which are independent of θ will survive the integration in the numerators. Therefore $\varphi^{(l)}(\theta)$ in the numerators of (2.1) may be replaced by the constants:

$$\varphi_{\text{symm}}^{(l)} \equiv \int_0^{2\pi} d\theta \varphi^{(0)\dagger}(\theta) \varphi^{(l)}(\theta) = \frac{1}{2} \sum_{i=0}^{\infty} \gamma_{0,i}^{(l)} \lambda^i, \quad (2.7)$$

the factor 1/2 reflecting the special normalization of $\varphi^{(0)}(\theta)$. The denominators of (2.1) become explicitly

$$\int_0^{\pi} d\theta \varphi^{(l)\dagger}(\theta) \varphi^{(l)}(\theta) = \sum_i \left(|\gamma_{0,i}^{(l)}|^2/2 + \sum_{l'} |\gamma_{l',i}^{(l)}|^2 \right) \lambda^{2i}, \quad (2.8)$$

where the sum over i is limited by the power of λ^2 up to which we want to carry the perturbation series; also l' is restricted to a finite number of terms, because of a band-diagonal structure of the $\gamma_{l',i}^{(l)}$ (see [1]). Extracting the coefficients of the power expansion in λ from (2.1) we obtain all desired moments of the end-to-end distribution, the lowest two being:

$$\langle R^2 \rangle = 2 \left\{ \xi L - \xi^2 \left[1 - e^{-L/\xi} \right] \right\}, \quad (2.9)$$

$$\begin{aligned} \langle R^4 \rangle &= 8L^2 \xi^2 - L \xi^3 \left(30 + \frac{40}{3} e^{-L/\xi} \right) \\ &+ \xi^4 \left(\frac{87}{2} - \frac{392}{9} e^{-L/\xi} + \frac{1}{18} e^{-4L/\xi} \right). \end{aligned} \quad (2.10)$$

The calculation of higher moments is straightforward with a Mathematica program, which we have placed on the internet in notebook form [7]. The above lowest moments agree with those in Ref. [4].

III. END-TO-END DISTRIBUTION

As in the previous paper, we shall now set up an analytic distribution function for $p_L(r) \equiv P_L(\mathbf{R})$, where $r = R/L$:

$$p_L(r) = (a_0 + a_2 x^2 + a_4 x^4 + a_6 x^6) x^k (1 - x^\beta)^m. \quad (3.1)$$

The parameters $a_0, \dots, a_6, k, \beta, m$ are functions of ξ/L and are determined by forcing the moments of (3.1),

$$\langle R^{2n} \rangle = L^{2n} \int_0^1 r^{2n+1} p_L(r) dr, \quad (3.2)$$

to fit the exact moments in the range $0 \leq n \leq \text{Max}(6, 10 \xi/L)$. For floppy chains with $\xi < 1$ we set $k = 0$; for very floppy chains with $\xi < 1/20$ the choice $a_2 = a_4 = a_6 = 0$ guarantees excellent accuracy. A comparison of $p_L(r)$ with Monte-Carlo data is shown in Fig. 1, and with higher resolution near $\mathbf{R} = 0$ in Fig. 2. The associated coefficients are listed in Table I. The

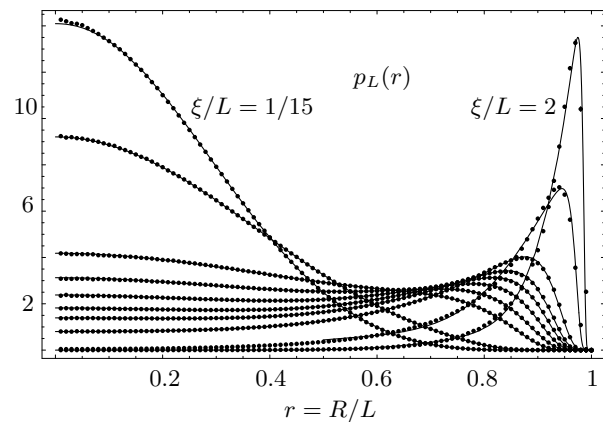


FIG. 1: End-to-end distribution $p_L(r)$ in $D = 2$ dimensions as a function of $r = R/L$ for various values of the stiffness $\xi/L = 1/15, 1/10, 1/5, 1/4, 3/10, 7/20, 2/5, 1/2, 1, 2$. The solid curves show the model functions (3.1) with parameters from Table I. The dots show the Monte Carlo data.

calculation of the coefficients in (3.1) requires some care to guarantee sensitivity to possible local minima, and to avoid running into unphysical oscillations. The latter may arise from the existence of polynomials in which all moments lower than some n vanish. Such oscillations are avoided by controlling the high moments and using only low polynomial coefficients in (3.1). For $\xi > 1/20$, a more involved strategy is necessary to avoid low-quality local solutions. We proceed as follows:

$\hat{\xi}$	a_0	a_2	a_4	a_6	k	m	β
1/400	400.0	0	0	0	0	196.784	1.99496
1/100	100.0	0	0	0	0	47.5378	1.98197
1/50	50.0	0	0	0	0	22.9930	1.97564
1/30	29.5302	-58.9195	77.9373	-87.3526	0	12.0224	2.00505
1/15	14.0952	-29.8504	66.8842	-68.1985	0	5.62896	2.21169
1/10	9.20629	-34.7515	50.6223	-26.2289	0	13.2737	10.5486
1/5	4.18239	-7.45808	11.616	-7.30855	0	10.2031	16.6444
1/4	3.12655	-4.9930	13.1086	-10.0222	0	9.42195	20.0750
3/10	2.38054	-3.38168	12.8823	-9.51483	0	9.16782	23.0164
7/20	1.82132	-2.062292	11.2343	-7.24306	0	8.84230	25.5206
2/5	1.39171	-0.952158	8.94986	-4.33545	0	8.49552	27.9120
1/2	0.800939	0.647524	4.36711	1.36933	0	8.06681	33.2814
1	42.8376	-173.308	263.327	-123.515	4.9880	11.4933	85.8428
2	504.624	-1832.52	2271.51	-925.829	13.4792	30.4949	244.143

TABLE I: Coefficients of the analytic distribution function for $p_L(r)$ in Eq. (3.1) for various values of the persistence length $\hat{\xi}$. They are obtained by making six or seven even moments of $p_L(r)$ agree with the exact ones.

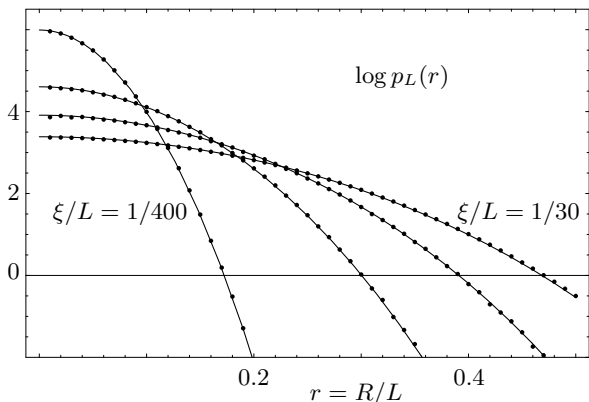


FIG. 2: End-to-end distribution near $\mathbf{R} = 0$ in $D = 2$ dimensions plotted logarithmically as a function of $r = R/L$ for various values of the stiffness for floppy polymers with $\xi/L = 1/400, 1/100, 1/50, 1/30$. The solid curves show the model functions (3.1) with parameters from Table I. The dots represent Monte Carlo data.

- In a first step we set $a_2 = a_4 = a_6 = 0$, $\beta = 2$, and determine preliminary values for k and m by fitting two higher moments of n near $10 \xi/L$. The first coefficient a_0 is fixed by normalization. This gives a reasonable starting value for m .
- In a second step, we introduce one more of the higher moments and improve the solution for k , m , and β .
- Next we solve for the coefficients a_j by bringing yet more moments into play. If $\xi/L < 1$, we take

$k = 0$ and solve for the a_j , keeping β and m fixed, based on four properly chosen moments. Then we solve for β and m keeping the a_j fixed, based on a choice of two moments. This alternating procedure is repeated three times. Finally, we solve for the a_j , β , and m simultaneously, based on six properly chosen moments.

- For $\xi/L \geq 1$, we proceed similarly, but allow for $k \neq 0$. The search for good coefficients a_j alternating with a search for good k , β , and m is repeated until it converges, with no further attempt to solve once more for all seven parameters simultaneously.

We check the quality of our simple distribution function (3.1) with the parameters of Table I by calculating its moments and comparing them with the exact ones. The comparison is shown in Table II for a large range of the persistence length ξ . As a measure of the quality of approximation we use the quantity Σ , listed in the second column of Table II, which sums up all squared deviations of the moments of the model from the exact ones in a relevant range of ξ :

$$\Sigma(\xi) = \sqrt{\sum_{n=0}^N (\langle R^{2n} \rangle_{p_L} - \langle R^{2n} \rangle_{P_L})^2}, \quad (3.3)$$

where we have extended the sum up to the moments of order $N = 12$ for $\xi/L < 1/5$, and $N = 24$ for $\xi/L \geq 1/5$.

Let us also convince ourselves of the high accuracy of our Monte Carlo data for the end-to-end distribution in Figs. 1 and 2 by listing the maximal deviation

$$\Delta_{\text{abs}} = \sup_{n=0}^{\infty} |\langle R^{2n} \rangle_{MC} - \langle R^{2n} \rangle_{P_L}| \quad (3.4)$$

ξ/L	Σ	Δ_{abs}	$\Delta_{\text{rel}}(N_{\text{max}})$
1/400	3×10^{-12}	0.000 126	0.9%(16)
1/100	2×10^{-13}	0.000 033	8%(16)
1/50	1×10^{-10}	0.000 071	1%(16)
1/30	5×10^{-9}	0.000 717	8%(16)
1/15	2×10^{-6}	0.000 057	0.9%(16)
1/10	5×10^{-5}	0.000 038	0.8%(24)
1/5	4×10^{-5}	0.000 048	0.5%(24)
1/4	9×10^{-5}	0.000 048	0.4%(24)
3/10	13×10^{-5}	0.000 047	0.3%(24)
7/20	2×10^{-4}	0.000 087	0.8%(36)
2/5	2×10^{-4}	0.000 100	0.8%(36)
1/2	2×10^{-4}	0.000 139	0.8%(36)
1	2×10^{-4}	0.000 217	0.4%(48)
2	8×10^{-5}	0.004 705	1.6%(48)

TABLE II: To illustrate the accuracy of our analytic approximation (3.1) of the end-to-end distribution we list the quantity Σ of Eq. (3.3) which measures the deviation of the even moments from the exact ones. The other two columns illustrate the accuracy of the Monte Carlo data for the end-to-end distribution by listing the maximal deviation Δ_{abs} of its moments and the relative deviation $\Delta_{\text{rel}}(N_{\text{max}})$ up to the moment N_{max} .

of its moments and the relative deviation

$$\Delta_{\text{rel}}(N_{\text{max}}) = \sup_{n=0}^{N_{\text{max}}} |\langle R^{2n} \rangle_{MC} / \langle R^{2n} \rangle_{PL} - 1| \quad (3.5)$$

up to the moment N_{max} .

Remarkably, in spite of the simplicity of the model, it is a nontrivial task to obtain accurate Monte Carlo results for $P_L(\mathbf{R})$ near $\mathbf{R} = 0$ which are sensitively displayed in the plots of Fig. 1 but which are almost ignored by the moments. The reason for the difficulty is the small configuration space for the small- \mathbf{R} data since the binning of the data is done in R to estimate the density $P_L(\mathbf{R})$. One is caught in the competition between large systematic errors resulting from a too large bin size ΔR , and statistical errors from a too small ΔR . As a compromise we employed in our simulations a uniform bin size $\Delta R/L = 0.01$ which in combination with a single-cluster update procedure and a statistics of 10^8 sampled chains yielded satisfactory accuracy near $\mathbf{R} = 0$, as shown in the high-resolution plot in Fig. 2.

Acknowledgment

This work was partially supported by ESF COSLAB Program and by the Deutsche Forschungsgemeinschaft under Grant Kl-256. WJ acknowledges partial support by the German-Israel-Foundation (GIF) under contract No. I-653-181.14/1999.

-
- [1] B. Hamprecht and H. Kleinert, *End-To-End Distribution Function of Stiff Polymers for all Persistence Lengths*, cond-mat/0305226.
- [2] J. Wilhelm and E. Frey, Phys. Rev. Lett. **77**, 2581 (1996).
- [3] H.E. Daniels, Proc. Roy. Soc. Edinburgh **63A**, 29 (1952). For details see also Chapter 15 of the textbook [5].
- [4] A. Dhar and D. Chaudhuri, Phys. Rev. Lett **89**, 065502 (2002).
- [5] H.Kleinert, *Path Integrals in Quantum Mechanics, Statistics and Polymer Physics* (World Scientific, Singapore, 1995) (<http://www.physik.fu-berlin.de/~kleinert/b5>).

- [6] See Appendices of Chapter 3 in the textbook [5], and the article by B. Hamprecht and A. Pelster in: *Fluctuating Paths and Fields - Festschrift Dedicated to Hagen Kleinert on the Occasion of his 60th Birthday*, Eds. W. Janke, A. Pelster, H.-J. Schmidt, and M. Bachmann (World Scientific, Singapore, 2001), p. 347.
- [7] The Mathematica notebook can be obtained from <http://www.physik.fu-berlin.de/~kleinert/b5/pgm15>.